J. Fluid Mech. (1996), *vol.* 322, *pp.* 147–163

Resonance gas oscillations in closed tubes

By A. GOLDSHTEIN, P. VAINSHTEIN, M. FICHMAN AND C. GUTFINGER

Faculty of Mechanical Engineering, Technion-Israel Institute of Technology, Haifa 32000, Israel

(Received 6 July 1995 and in revised form 10 April 1996)

The problem of gas motion in a tube closed at one end and driven at the other by an oscillating piston is studied theoretically. When the piston vibrates with a finite amplitude at the first acoustic resonance frequency, periodic shock waves are generated, travelling back and forth in the tube. A perturbation method, based on a small Mach number, M and a global mass conservation condition, is employed to formulate a solution of the problem in the form of two standing waves separated by a jump (shock front). By expanding the equations of motion in a series of a small parameter $\epsilon = M^{1/2}$, all hydrodynamic properties are predicted with an accuracy to second-order terms, i.e. to ϵ^2. It is found that the first-order solution coincides with the previous theories of Betchov (1958) and Chester (1964), while additional terms predict a non-homogeneous time-averaged pressure along the tube. This prediction compares favourably with experimental results from the literature. The importance of the phenomenon is discussed in relation to different transport processes in resonance tubes.

1. Introduction

The present paper considers gas oscillations produced by an oscillating piston at one end of a closed tube. Experimental evidence (Saenger & Hadson 1960) shows that in a closed tube, a piston vibrating in a narrow frequency band around a resonance frequency can amplify the gas oscillations to the extent that the shock waves develop. The latter travel back and forth between the piston surface and the rigid end. In order to explain this observation, Betchov (1958) and Saenger & Hudson (1960) constructed theoretical models based on the existence of a propagating shock discontinuity.

Saenger & Hudson's solution is flawed by the fact that the amplitude of gas oscillations becomes infinite in the absence of shear viscosity and heat conduction. Betchov was the first to show that even if shear viscosity and heat conduction are negligible, nonlinear cumulative effects lead to finite gas oscillations in closed tubes. He found that for small displacements of the piston an oscillatory flow consists of two simple waves, having the same frequency, separated by a jump. This solution is interesting in that although the oscillations remain small the velocity in the gas is much higher than that of the piston, yet still much smaller than the speed of sound. Betchov also discusses the modifying effect of wall friction on his solution, assuming, as did Saenger & Hudson (1960), that this effect is equivalent to a body force proportional to the velocity. In both references it is suggested that wall friction could significantly modify the solution.

Chester (1964) has developed a consistent theory of gas oscillations in a closed tube near resonance, predicting the appearance and strength of the shock waves. He used a combination of the method of characteristics and a straightforward expansion, to obtain a solution accounting for compressive and shear viscosity in the boundary layer near the tube wall. For typical laboratory conditions the effect of compressive viscosity

was shown to be small in contrast to that of shear viscosity. Chester's theory is more general in the sense that shock waves appear as a natural outcome of the solution when the piston frequency approaches one of the resonant frequencies. Outside these narrow resonant bands, the solution is continuous but not purely harmonic. This work was further extended by Keller (1976) to include the effect of boundary-layer friction. Other related studies on closed resonance tubes were reported by Cruikshank (1972), Merkli & Thomann (1975), Zaripov & Ilhamov (1976), Ochmann (1985) and Ockendon *et al.* (1993).

It is noted that, with exception of Ochmann (1985), all the early investigators consider only quasi-steady oscillations. Ochmann (1985) studied transient effects in closed resonance tubes, exited by distributed forces, employing the method of averaging to describe the slowly varying wave amplitude. More recently, Wang & Kassoy (1995) have investigated the piston-driven resonances in a gas column, subject to a variety of boundary conditions. In order to study the evolution of the wave field in a cylinder subject to small-amplitude piston oscillations, they developed a mathematical technique that combines a formal multi-scale perturbation procedure with Fourier series expansions. This technique, which is based on an initial-boundary-value formulation, has the advantage of being fully applicable for treatment of the nonlinear evolution to the limit cycle for both closed and open end conditions. At the steady-state limit both theories approach that of Chester.

Several attempts have been made to compare experimental measurements of the shape of the pressure wave with theoretical predictions of Chester. The most thorough comparison was performed by Cruikshank (1972), who showed that Chester's theory is valid only for a limited range of driving amplitudes. For these amplitudes experimental and theoretical waveforms are in good quantitative agreement. For sufficiently small values of the amplitude parameter ϵ, which is proportional to the square root of the Mach number, $M^{1/2}$, characterizing the ratio of gas velocity immediately on the piston and the speed of sound, the motion of the gas is shockless or is accompanied by weak shock waves of the order of ϵ^2. For larger values of ϵ, experiments revealed amplitude discrepancies, despite the general shape similarities.

Several theoretical papers investigate this problem for a range of driving amplitudes where Chester's theory is invalid. These papers consider mostly timescales long compared with the acoustic timescale (Klein & Peters 1988; Wang & Kassoy, 1990; and studies cited therein). In these studies the formation of a weak shock wave for non-resonant frequencies from an initially continuous compression wave were investigated by different multi-scale perturbation methods. The analyses were limited only to waves, whose amplitudes are comparable with the small Mach number.

The present one-dimensional study is concerned with the explicit effects of gas dynamic processes on equilibrium compression and expansion. In this sense the effects of non-planar flow (e.g. vortices) are not addressed, although they inevitably occur in realistic situations. The initial-value problem of the interaction of a sound wave with vorticity and entropy waves was considered by Majda & Rosales (1984), and Majda, Rosales & Shonbeck (1988). The new results of resonant acoustics obtained include substantial, almost periodic exchange of energy between the nonlinear sound waves, the existence of the smooth periodic wavetrains, and the role of such smooth wave patterns in eliminating or suppressing the strong temporal decay of sawtooth profile solutions. They found that smooth initial data with sufficiently small amplitudes never develop shocks throughout a long time interval.

Our work considers the externally driven gas column as in resonance studies conducted by Betchov (1958) and Chester (1964), when limiting-cycle oscillations are

accompanied by travelling shock waves of the order of ϵ. These oscillations are characterized by a balance between energy input by the driving piston and internal dissipation by the shock waves. Entropy changes induced by the $O(\epsilon)$ shock, which occur at the $O(\epsilon^3)$ level, have no influence on the process for times less than T/ϵ, where T is the period of external oscillations. This restriction is standard for limiting-cycle problems. For the problem of a shock wave of order M entropy perturbation analysis was performed by Klein & Peters (1988).

In the works of Galiev *et al.* (1970) and Zaripov & Ilhamov (1976) different nonlinear solutions are obtained and some experiments performed for amplitudes larger than those of Chester's theory. For example, it follows from the experimental data of Zaripov & Ilhamov that the time-averaged pressure at the plug is larger than that in the gas at the initial state (see also Saenger & Hudson 1960). Still, there are experimental effects which until now had no theoretical explanation. For instance, the experiments of Merkli & Thomann (1975) show that there is a variation of the time-averaged pressure along the tube.

The present work considers the theory of one-dimensional, nonlinear oscillations in an inviscid gas inside a closed tube. The theory neither describes resonant wave amplifications nor formations of shock waves. It is restricted to a time periodic steady state and is valid as long as entropy perturbations and viscous boundary-layer effects are neglected. These restrictions make it possible to consider amplified periodic gas oscillations which occur over many cycles, when the gas 'forgets' its initial conditions. An analytical solution at resonance frequency is obtained in terms of asymptotic expansions in the small parameter ϵ. The first term of the asymptotic expansion coincides with the solution of Betchov, while the higher-order terms account for the effects of average pressure increase at the plug, and non-homogeneous pressure distribution along the tube.

2. Basic equations

2.1. *Problem formulation*

We consider one-dimensional inviscid motion of an ideal gas, for which the equations of motion are:

$$\frac{\partial u}{\partial t}+u\frac{\partial u}{\partial x}+\frac{1}{\rho}\frac{\partial P}{\partial x}=0, \quad \frac{\partial \rho}{\partial t}+\rho\frac{\partial u}{\partial x}+u\frac{\partial \rho}{\partial x}=0, \tag{1a, b}$$

where P is given by the following constitutive equation:

$$P = A\rho^{\gamma}, \tag{2}$$

here γ is the adiabatic exponent and A is constant for an isentropic process. We neglect the change of entropy during the considered process.

Let ρ_0 and C_0 be the initial gas density and speed of sound, respectively, with the general relations

$$C_0^2 = \gamma\frac{P}{\rho}\Big|_{\substack{\rho=\rho_0 \\ s=const}} = \gamma A\rho_0^{\gamma-1}. \tag{3}$$

We consider a long tube closed at one end ($x = 0$) with an oscillating piston at the other end ($x = L$). The motion of the piston is sinusoidal with a frequency ω and a velocity amplitude u_0. The boundary conditions may be written in the following form:

$$u(x, t) = 0 \quad \text{at} \quad x = 0, \tag{4a}$$

$$u(x, t) = \dot{x}_p(t) \quad \text{at} \quad x = x_p(t), \tag{4b}$$

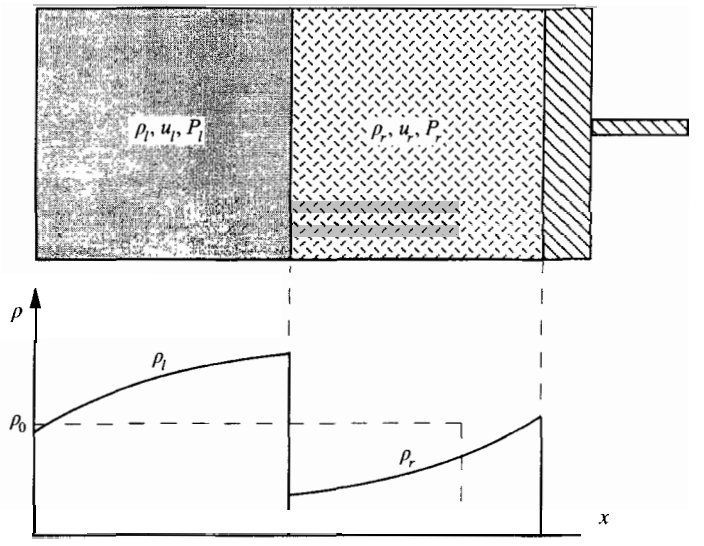

where $x_p(t)$, $\dot{x}_p(t)$ are the coordinate and velocity of the piston, respectively,

$$x_p(t) = L + \frac{u_0}{\omega}\sin(\omega t), \quad \dot{x}_p(t) = u_0\cos(\omega t). \tag{5a, b}$$

Since the problem includes a shock wave, a condition at the shock front is needed. For the inviscid perfect gas the jump conditions may be written in the following Rankine–Hugoniot form:

$$\rho_l(U-u_l) = \rho_r(U-u_r), \tag{6a}$$

$$\rho_l(U-u_l)^2 + P_l = \rho_r(U-u_r)^2 + P_r, \tag{6b}$$

where indexes l, r refer to the respective values at the left-hand and right-hand sides of the shock front X_u moving with speed U (see figure 1).

Usually the jump conditions define the position of the shock front. Here, however, this is not the case, and an additional condition is needed. For example, Galiev, Ilhamov & Sadykov (1970) used the condition of mass conservation at any cross-section of the tube. In the present study we use the global condition of mass conservation within the tube. In our notation this condition may be written as follows (see figure 1):

$$\int_0^{X_u(t)} \rho_l(x,t)\,\mathrm{d}x + \int_{X_u(t)}^{x_p(t)} \rho_r(x,t)\,\mathrm{d}x = \rho_0 L. \tag{7}$$

2.2. *Problem reduction*

Let us introduce the following dimensionless variables and functions

$$\left.\begin{aligned} \tilde{x} &= x\omega/C_0, \quad \tilde{t} = t\omega, \\ \tilde{u} &= u/C_0, \quad \tilde{\rho} = \rho/\rho_0. \end{aligned}\right\} \tag{8}$$

Using these dimensionless values, (1), (2) may be written in the dimensionless form as

$$\frac{\partial\tilde{u}}{\partial\tilde{t}} + \tilde{u}\frac{\partial\tilde{u}}{\partial\tilde{x}} + \tilde{\rho}^{\gamma-2}\frac{\partial\tilde{\rho}}{\partial\tilde{x}} = 0, \quad \frac{\partial\tilde{\rho}}{\partial\tilde{t}} + \tilde{\rho}\frac{\partial\tilde{u}}{\partial x} + \tilde{u}\frac{\partial\tilde{\rho}}{\partial\tilde{x}} = 0. \tag{9a, b}$$

and the boundary conditions (4*a*, *b*) become

$$\tilde{u}(\tilde{t}, \tilde{x}) = 0 \qquad \text{at} \quad \tilde{x} = 0, \tag{10a}$$

$$\tilde{u}(\tilde{t}, \tilde{x}) = \dot{\tilde{x}}_p(\tilde{t}) \quad \text{at} \quad \tilde{x} = \tilde{x}_p(\tilde{t}). \tag{10b}$$

Here $\tilde{x}_p(\tilde{t})$, $\dot{\tilde{x}}_p(\tilde{t})$ are the dimensionless coordinate and speed of piston, respectively,

$$\tilde{x}_p(\tilde{t}) = \tilde{L} + \epsilon^2 \sin \tilde{t}, \quad \dot{\tilde{x}}_p(\tilde{t}) = \epsilon^2 \cos \tilde{t}, \tag{11a, b}$$

where $\tilde{L} = L\omega/C_0$ is the dimensionless length of the tube, while the dimensionless parameter ϵ is the square root of the Mach number, $\epsilon^2 = u_0/C_0 = M$.

Restricting the analysis to the case of small ϵ, i.e. $\epsilon \ll 1$, we seek a solution of (9*a*, *b*) in the form of the following expansions

$$\tilde{\rho} = 1 + \epsilon\tilde{\rho}^{(1)} + \epsilon^2\tilde{\rho}^{(2)} + O(\epsilon^3), \tag{12a}$$

$$\tilde{u} = \epsilon\tilde{u}^{(1)} + \epsilon^2\tilde{u}^{(2)} + O(\epsilon^3), \tag{12b}$$

$$\tilde{P} = \frac{\tilde{\rho}^\gamma}{\gamma} = \frac{1}{\gamma} + \epsilon\tilde{\rho}^{(1)} + [\tilde{\rho}^{(2)} + \tfrac{1}{2}(\gamma - 1)(\tilde{\rho}^{(1)})^2]\epsilon^2 + O(\epsilon^3). \tag{12c}$$

Substitution of expansions (12*a*, *b*) into (9*a*, *b*) yields:

First approximation

$$\frac{\partial\tilde{u}^{(1)}}{\partial\tilde{t}} + \frac{\partial\tilde{\rho}^{(1)}}{\partial\tilde{x}} = 0, \quad \frac{\partial\tilde{\rho}^{(1)}}{\partial\tilde{t}} + \frac{\partial\tilde{u}^{(1)}}{\partial\tilde{x}} = 0, \tag{13a, b}$$

Second approximation

$$\frac{\partial\tilde{u}^{(2)}}{\partial\tilde{t}} + \frac{\partial\tilde{\rho}^{(2)}}{\partial\tilde{x}} = -\tilde{u}^{(1)}\frac{\partial\tilde{u}^{(1)}}{\partial\tilde{x}} - (\gamma - 2)\tilde{\rho}^{(1)}\frac{\partial\tilde{\rho}^{(1)}}{\partial\tilde{x}}, \tag{14a}$$

$$\frac{\partial\tilde{\rho}^{(2)}}{\partial\tilde{t}} + \frac{\partial\tilde{u}^{(2)}}{\partial\tilde{x}} = -\tilde{\rho}^{(1)}\frac{\partial\tilde{u}^{(1)}}{\partial\tilde{x}} - \tilde{u}^{(1)}\frac{\partial\rho^{(1)}}{\partial\tilde{x}}. \tag{14b}$$

The expansion of the boundary conditions given by (10) and (11) yields:

First approximation

$$\tilde{u}^{(1)}_{|\tilde{x}=0} = 0, \quad \tilde{u}^{(1)}_{|\tilde{x}=\tilde{L}} = 0, \tag{15a, b}$$

Second approximation

$$\tilde{u}^{(2)}_{|\tilde{x}=0} = 0, \quad \tilde{u}^{(2)}_{|\tilde{x}=\tilde{L}} = \cos\tilde{t}. \tag{16a, b}$$

Using the constitutive equation (2) together with relations (8), the jump conditions given by (6) may be written in the dimensionless form as

$$\tilde{\rho}_l(\tilde{t}, \tilde{X}_u(\tilde{t}))(\tilde{U}(\tilde{t}) - \tilde{u}_l(\tilde{t}, \tilde{X}_u(\tilde{t}))) = \tilde{\rho}_r(\tilde{t}, \tilde{X}_u(\tilde{t}))(\tilde{U}(\tilde{t}) - \tilde{u}_r(\tilde{t}, \tilde{X}_u(\tilde{t}))), \tag{17a}$$

$$\tilde{\rho}_l(\tilde{t}, \tilde{X}_u(\tilde{t}))(\tilde{U}(\tilde{t}) - \tilde{u}_l(\tilde{t}, \tilde{X}_u(\tilde{t})))^2 + \frac{\tilde{\rho}_l^\gamma(\tilde{t}, \tilde{X}_u(\tilde{t}))}{\gamma}$$
$$= \tilde{\rho}_r(\tilde{t}, \tilde{X}_u(\tilde{t}))(\tilde{U}(\tilde{t}) - \tilde{u}_r(\tilde{t}, \tilde{X}_u(\tilde{t})))^2 + \frac{\tilde{\rho}_r^\gamma(\tilde{t}, \tilde{X}_u(\tilde{t}))}{\gamma}, \tag{17b}$$

Because the Mach number M, and/or the parameter ϵ, are small, the hypothesis of a

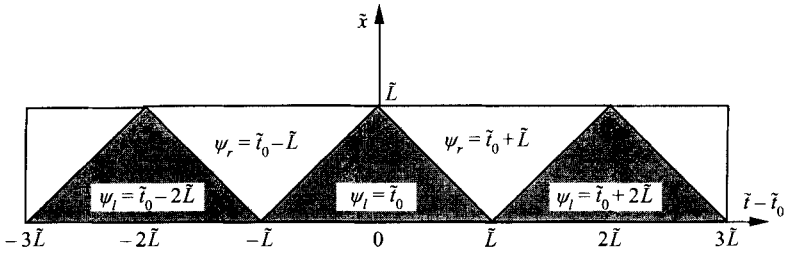

FIGURE 2. The oscillating shock wave.

weak shock wave is valid and, hence, the dimensionless shock wave speed, $\tilde{U}(\tilde{t})$ and the coordinate of the shock front, $\tilde{X}_u(\tilde{t})$ may be expanded in the following series:

$$\tilde{U}(\tilde{t}) = \tilde{U}^{(0)}(\tilde{t}) + \epsilon\tilde{U}^{(1)}(\tilde{t}) + \epsilon^2\tilde{U}^{(2)}(\tilde{t}) + O(\epsilon^3), \tag{18a}$$

$$\tilde{X}_u(\tilde{t}) = \tilde{X}_u^{(0)}(\tilde{t}) + \epsilon\tilde{X}_u^{(1)}(\tilde{t}) + \tilde{X}_u^{(2)}(\tilde{t}) + O(\epsilon^3), \tag{18b}$$

where

$$\frac{\mathrm{d}}{\mathrm{d}\tilde{t}}\tilde{X}_u^{(i)}(\tilde{t}) = \tilde{U}^{(i)}(\tilde{t}) \quad (i = 0, 1, 2, \ldots), \tag{18c}$$

and $\tilde{U}^{(0)}(\tilde{t}) = 1$ for a shock wave travelling from left to right (see figure 2) and $\tilde{U}^{(0)}(\tilde{t}) = -1$ for a shock wave travelling from the right-hand side to the left-hand side. Substitution of series (18*a*, *b*), (12) into the jump conditions (17) and expansion in a series with respect the small parameter ϵ yields:

First approximation

$$\tilde{U}^{(0)}(\tilde{t})\,\tilde{\rho}_l^{(1)}(\tilde{t},\tilde{x}) - \tilde{u}_l^{(1)}(\tilde{t},\tilde{x}) = \tilde{U}^{(0)}(\tilde{t})\,\tilde{\rho}_r^{(1)}(\tilde{t},\tilde{x}) - \tilde{u}_r^{(1)}(\tilde{t},\tilde{x})|_{\tilde{x}=\tilde{X}_u^{(0)}(\tilde{t})}, \tag{19}$$

Second approximation

$$\tilde{U}^{(1)}(\tilde{t}) = \tfrac{1}{4}(\gamma-1)\,(\tilde{\rho}_r^{(1)}(\tilde{t},\tilde{x}) + \tilde{\rho}_l^{(1)}(\tilde{t},\tilde{x}))\,\tilde{U}^{(0)}(\tilde{t}) + \tfrac{1}{2}(\tilde{u}_r^{(1)}(\tilde{t},\tilde{x}) + \tilde{u}_l^{(1)}(\tilde{t},\tilde{x}))|_{\tilde{x}=\tilde{X}_u^{(0)}(\tilde{t})}, \tag{20a}$$

$$\begin{aligned}
&\Big\{\tilde{U}^{(0)}(\tilde{t})\,\tilde{\rho}_l^{(2)}(\tilde{t},\tilde{x}) - \tilde{u}_l^{(2)}(\tilde{t},\tilde{x}) + \tilde{\rho}_l^{(1)}(\tilde{t},\tilde{x})\,[\tilde{U}^{(1)}(\tilde{t}) - \tilde{u}_l^{(1)}(\tilde{t},\tilde{x})] \\
&\qquad + \tilde{X}_u^{(1)}(\tilde{t})\frac{\partial}{\partial x}[\tilde{U}^{(0)}(\tilde{t})\,\tilde{\rho}_l^{(1)}(\tilde{t},\tilde{x}) - \tilde{u}_l^{(1)}(\tilde{t},\tilde{x})]\Big\}_{\tilde{x}=\tilde{X}_u^{(0)}(\tilde{t})} \\
&= \Big\{\tilde{U}^{(0)}(\tilde{t})\,\tilde{\rho}_r^{(2)}(\tilde{t},\tilde{x}) - \tilde{u}_r^{(2)}(\tilde{t},\tilde{x}) + \tilde{\rho}_r^{(1)}(\tilde{t},\tilde{x})\,[\tilde{U}^{(1)}(\tilde{t}) - \tilde{u}_r^{(1)}(\tilde{t},\tilde{x})] \\
&\qquad + \tilde{X}_u^{(1)}(\tilde{t})\frac{\partial}{\partial x}[\tilde{U}^{(0)}(\tilde{t})\,\tilde{\rho}_r^{(1)}(\tilde{t},\tilde{x}) - \tilde{u}_r^{(1)}(\tilde{t},\tilde{x})]\Big\}_{\tilde{x}=\tilde{X}_u^{(0)}(\tilde{t})}.
\end{aligned} \tag{20b}$$

Note that equations (19), (20) are written at the zeroth approximation, $\tilde{X}_u^{(0)}(\tilde{t})$ of the shock front $\tilde{X}_u(\tilde{t})$. We will show later that the first-order solution turns (19) into an identity for any shock front position. Therefore, an additional condition for the determination of the shock front position is need. For this purpose, the condition of mass conservation (7) is used.

Normalized mass conservation condition

Using expansion of the gas density (12*a*) together with relations (8), the mass conservation condition (7) may be written in dimensionless form

$$\int_0^{\tilde{X}_u(\tilde{t})} [1 + \epsilon\tilde{\rho}_l^{(1)}(\tilde{t},\tilde{x}) + \epsilon^2\tilde{\rho}_l^{(2)}(\tilde{t},\tilde{x})]\,\mathrm{d}\tilde{x} + \int_{\tilde{X}_u(\tilde{t})}^{\tilde{x}_p(\tilde{t})} [1 + \epsilon\tilde{\rho}_r^{(1)}(\tilde{t},\tilde{x}) + \epsilon^2\tilde{\rho}_r^{(2)}(\tilde{t},\tilde{x})]\,\mathrm{d}\tilde{x} = \tilde{L} + O(\epsilon^3).$$

After substitution of the equation of motion for the piston (11*a*) and of the expansion of the shock front (18*a*) into the above mass conservation condition one can expand it in a series with respect to the small parameter ϵ. The density in the expansion of (12*a*) is normalized by the initial density ρ_0 (see equation (8)) in such a way that all the mass of the gas is included in the zeroth-order term. Therefore, each perturbation of the homogeneous (zeroth-order) solution should have no contribution to the total mass of the gas. As a result, the mass normalization condition for densities $\tilde{\rho}^{(1)}$, $\tilde{\rho}^{(2)}$ is obtained as:

$$\int_0^{\tilde{X}_u^{(0)}(\tilde{t})} \tilde{\rho}_l^{(1)}(\tilde{t},\tilde{x})\,\mathrm{d}\tilde{x} + \int_{\tilde{X}_u^{(0)}(\tilde{t})}^{\tilde{L}} \tilde{\rho}_r^{(1)}(\tilde{t},\tilde{x})\,\mathrm{d}\tilde{x} = 0, \tag{21a}$$

$$\sin\tilde{t} + \int_0^{\tilde{X}_u^{(0)}(\tilde{t})} \tilde{\rho}_l^{(2)}(\tilde{t},\tilde{x})\,\mathrm{d}\tilde{x} + \int_{\tilde{X}_u^{(0)}(\tilde{t})}^{\tilde{L}} \tilde{\rho}_r^{(2)}(\tilde{t},\tilde{x})\,\mathrm{d}\tilde{x} = [\tilde{\rho}_l^{(1)}(\tilde{t},\tilde{X}_u^{(0)}(\tilde{t})) - \tilde{\rho}_r^{(1)}(\tilde{t},\tilde{X}_u^{(0)}(\tilde{t}))]\,\tilde{X}_u^{(1)}(\tilde{t}). \tag{21b}$$

Equation (21*a*) does not take into account the oscillation of the piston and the initial density of the gas. This equation shows that the total area of the left-hand side and right-hand side densities (separated by a zeroth-order approximation of the shock front) is zero (see figure 1). Equation (21*b*) includes a term which describes the motion of the piston (first term in the left-hand side) and the contribution of the first-order terms of the solution (see the right-hand side), which reflect nonlinearity of the problem.

The problem formulated above is valid for a band of frequencies close to the first resonance frequency. We consider the resonance case, when the period of natural oscillations of the first-order problem, $2\tilde{L}$, is equal to the period of the oscillations of the piston, 2π, i.e.,

$$\tilde{L} = \pi. \tag{22}$$

3. First-order solution

3.1. *Mathematical model*

The general solution of the problem includes a discontinuity. We look for a solution comprised of two continuous parts, i.e. left-hand side and right-hand side parts separated by a shock front (see figure 1). In the first approximation each of the parts should satisfy equations (13*a*, *b*). Using indices *l*, *r* for the left-hand side and right-hand side parts (waves), the equations of motion become:

Left-hand side wave

$$\frac{\partial\tilde{u}_l^{(1)}}{\partial\tilde{t}} + \frac{\partial\tilde{\rho}_l^{(1)}}{\partial\tilde{x}} = 0, \quad \frac{\partial\tilde{\rho}_l^{(1)}}{\partial\tilde{t}} + \frac{\partial\tilde{u}_l^{(1)}}{\partial\tilde{x}} = 0, \tag{23a, b}$$

Right-hand side wave

$$\frac{\partial\tilde{u}_r^{(1)}}{\partial\tilde{t}} + \frac{\partial\tilde{\rho}_r^{(1)}}{\partial\tilde{x}} = 0, \quad \frac{\partial\tilde{\rho}_r^{(1)}}{\partial\tilde{t}} + \frac{\partial\tilde{u}_r^{(1)}}{\partial\tilde{x}} = 0. \tag{23c, d}$$

In this notation the boundary conditions (15) are replaced by

$$\tilde{u}_{l|\tilde{x}=0}^{(1)} = 0, \quad \tilde{u}_{r|\tilde{x}=\tilde{L}}^{(1)} = 0. \tag{24a, b}$$

One can see, that the motion of the piston is removed from the boundary conditions (24*a*, *b*). Consequently, in the first approximation the problem is reduced to the

problem of free oscillation of an inviscid gas bounded by two rigid walls. In the following section we consider the latter problem assuming that the solution may be presented in the form of two standing waves separated by a jump. This form of the solution was first presented by Betchov (1958).

3.2. *Analytical solution*

We look for a solution of the first-order problem represented by (23) and conditions (24) in Betchov's form, i.e.,

$$\tilde{u}_l^{(1)} = A_l \sin(\alpha_l \tilde{x}) \cos \alpha_l(\tilde{t} - \psi_l), \tag{25a}$$

$$\tilde{\rho}_l^{(1)} = -A_l \cos(\alpha_l \tilde{x}) \sin \alpha_l(\tilde{t} - \psi_l), \tag{25b}$$

$$\tilde{u}_r^{(1)} = A_r \sin \alpha_r(\tilde{x} - \tilde{L}) \cos \alpha_r(\tilde{t} - \psi_r), \tag{26a}$$

$$\tilde{\rho}_r^{(1)} = -A_r \cos \alpha_r(\tilde{x} - \tilde{L}) \sin \alpha_r(\tilde{t} - \psi_r). \tag{26b}$$

where A_l, A_r, α_l, α_r, ψ_l, ψ_r are constants to be calculated. Solution (25*a*, *b*) satisfies (23*a*, *b*) and condition (24*a*). Solution (26*a*, *b*) satisfies (23*c*, *d*) and condition (24*b*).

At any time t the left-hand standing wave given by solution (25) is placed between the left-hand rigid wall and the shock front, while the right-hand standing wave given by solution (26) is placed between the right-hand rigid wall and the shock front (see figure 1). Conditions at the shock front are given by (19). Substitution of solution (25*a*, *b*), (26*a*, *b*) into condition (19) yields

$$A_l \sin \alpha_l [\tilde{x} + (\tilde{t} - \psi_l) \tilde{U}^{(0)}(\tilde{t})] = A_r \sin \alpha_r [\tilde{x} - \tilde{L} + (\tilde{t} - \psi_r) \tilde{U}^{(0)}(\tilde{t})], \tag{27}$$

where $\tilde{x} = \tilde{X}_u^{(0)}(\tilde{t})$ is the shock front position, and $\tilde{U}^{(0)} = \tilde{U}^{(0)}(\tilde{t})$ is the shock front velocity in the zeroth approximation. Equation (27) yields

$$A_l = A_r = A\,(\text{say}), \quad \alpha_r = \alpha_l = \alpha\,(\text{say}), \quad \psi_l = \psi_r + \tilde{L}\tilde{U}^{(0)}. \tag{28a–c}$$

One can see that relations (28) turn (27) into an identity for all $\tilde{x}$, not only for $\tilde{x} = \tilde{X}_u^{(0)}(\tilde{t})$. It means that the first-order solution also satisfies the jump condition (19) for all $\tilde{x}$. Therefore, the last terms in the jump condition (20*b*) vanish.

3.3. *Periodical oscillations*

Equation (27) together with relations (28) does not determine the shock front position $\tilde{X}_u = \tilde{X}_u(\tilde{t})$. For this purpose we turn to the mass normalization condition (21*a*). After the substitution of relations (25*b*), (26*b*), (28*a–c*) into the latter condition and integration we obtain:

$$\sin \alpha(\tilde{t} - \psi_r) \sin \alpha [\tilde{X}_u^{(0)}(\tilde{t}) - \tilde{L}] - \sin \alpha(\tilde{t} - \psi_l) \sin \alpha [\tilde{X}_u^{(0)}(\tilde{t})] = 0. \tag{29}$$

It follows from (18*a–c*) that in the zeroth approximation the speed of the shock front is merely equal to ± 1 and the trajectories of the shock front follow a zigzag path. This path may be characterized by parameters ψ_l, ψ_r which also characterize solution (25) and (26). According to this solution, parameters ψ_l, ψ_r determine the times when the shock wave is reflected from the walls. It may be shown that these parameters are simply connected through a reflection time from the plug. At the time when the shock wave reflects from the plug, equation (29) reduces to

$$\sin \alpha(\tilde{t} - \psi_r) \sin \alpha \tilde{L} = 0, \tag{30a}$$

while for the reflection time from the wall $\tilde{x} = \tilde{L}$, equation (29) becomes

$$\sin \alpha(\tilde{t} - \psi_l) \sin \alpha \tilde{L} = 0. \tag{30b}$$

In the following section it is shown that

$$\sin \alpha \tilde{L} \neq 0. \tag{31}$$

Bearing in mind this condition and equations (30*a*, *b*), the physical sense of the parameters may be explained as follows: parameters ψ_l, ψ_r determine the times when the shock wave reflects from the walls $\tilde{x} = \tilde{L}$, 0, respectively, i.e.,

$$\tilde{X}_u^{(0)}(\psi_l) = \tilde{L}, \quad \tilde{X}_u^{(0)}(\psi_r) = 0. \tag{32a, b}$$

This may also be seen directly from (25*b*) and (26*b*) and from the normalization condition (21*a*). For example, at the instant $\tilde{t} = \psi_l$ according to condition (32*a*) the right-hand side solution (26*b*) does not affect the condition (21*a*). On the other hand, at that time the left-hand side density is equal to zero. Under these conditions of total mass conservation, all integrals in equation (21*a*) equal zero and, hence, the global mass conservation condition turns into identity.

Now we consider the shock-wave oscillation between the rigid walls $\tilde{x} = 0, \tilde{L}$ on the plane $\tilde{x}\tilde{t}$ (see figure 2). The shock front trajectory is comprised of straight segments inclined at angles $\pm\frac{1}{4}\pi$ which corresponds in the zeroth approximation to the shock waves propagating with speeds equal to ± 1, respectively. Each of the two straight segments together with the lines $\tilde{x} = 0, \tilde{L}$ comprise a triangle. The triangles lying on the line $\tilde{x} = 0$ correspond to the left-hand side waves, while those adjacent to the line $\tilde{x} = \tilde{L}$ correspond to the right-hand side solution. Within every triangle area the concomitant values ψ_l, ψ_r are constants; where ψ_l is the reflection time from the wall $\tilde{x} = \tilde{L}$, while ψ_r is the reflection time from the wall $\tilde{x} = 0$. According to relations (28*c*), (32*a*, *b*), each successive reflection occur after the same period $\tilde{L}$. Bearing in mind these considerations, solution (25), (26) shows that the oscillations of the shock wave are periodical with the period $2\tilde{L}$. Therefore, all values ψ_l, ψ_r may be expressed via the time $\tilde{t}_0$ (see figure 2), where

$$\tilde{X}_u(\tilde{t}_0) = \tilde{L}, \tag{33}$$

which is enough to describe the oscillation during the period $2\tilde{L}$.

Considering the interval $|\tilde{t} - t_0| \leqslant \tilde{L}$ and setting $\psi_l = \tilde{t}_0$ (see figure 2), solutions (25), (26) and (28) may be rewritten in the following form:

$$\tilde{u}_l^{(1)} = A \sin(\alpha\tilde{x}) \cos \alpha(\tilde{t} - \tilde{t}_0), \tag{34a}$$

$$\tilde{\rho}_l^{(1)} = -A \cos(\alpha\tilde{x}) \sin \alpha(\tilde{t} - \tilde{t}_0), \tag{34b}$$

$$\tilde{u}_r^{(1)} = A \sin \alpha(\tilde{x} - \tilde{L}) \cos \alpha(\tilde{t} - \tilde{t}_0 + \tilde{U}^{(0)}\tilde{L}), \tag{35a}$$

$$\tilde{\rho}_r^{(1)} = -A \cos \alpha(\tilde{x} - \tilde{L}) \sin \alpha(\tilde{t} - \tilde{t}_0 + \tilde{U}^{(0)}\tilde{L}), \tag{35b}$$

The speed of the shock front in the above expressions is

$$\tilde{U}^{(0)}(\tilde{t}) = \begin{cases} 1 & \text{for} \quad -\tilde{L} < \tilde{t} - \tilde{t}_0 < 0, \\ -1 & \text{for} \quad 0 < \tilde{t} - \tilde{t}_0 < \tilde{L}. \end{cases} \tag{36}$$

Substitution of (36) into (18*c*) with $i = 0$ and integration with initial condition (33) yields the trajectory of the shock front in the zeroth approximation:

$$X_u^{(0)}(\tilde{t}) = \int_{\tilde{t}_0}^{\tilde{t}} \tilde{U}^{(0)}(\tau)\, \mathrm{d}\tau = (\tilde{t} - \tilde{t}_0)\, \tilde{U}^{(0)}(\tilde{t}) + \tilde{L}. \tag{37}$$

We have shown in this section that the first-order solution (25) and (26) describes free periodic oscillations with a period $2\tilde{L}$. This solution contains three unknown parameters, A, $\tilde{t}_0, \alpha$. These parameters will now be determined from the condition of existence of the second-order periodic solution.

4. Second-order approximation of the problem

4.1. *Mathematical model*

Now we derive the governing equation for the second approximation of the left-hand side and right-hand side waves. Substitution of the first-order solution (35*a*, *b*) of the right-hand side wave into the right-hand sides of equations (14*a*, *b*) yields:

$$\frac{\partial \tilde{u}_r^{(2)}}{\partial \tilde{t}_r}+\frac{\partial \tilde{\rho}_r^{(2)}}{\partial \tilde{x}_r}=-R_0\sin\tilde{x}_r+C_0\sin\tilde{x}_r\cos\tilde{t}_r, \tag{38a}$$

$$\frac{\partial \tilde{\rho}_r^{(2)}}{\partial \tilde{t}_r}+\frac{\partial \tilde{u}_r^{(2)}}{\partial \tilde{x}_r}=B_0\sin\tilde{t}_r\cos\tilde{x}_r, \tag{38b}$$

where

$$\tilde{x}_r=2\alpha(\tilde{x}-\tilde{L}),\quad \tilde{t}_r=2\alpha(\tilde{t}-\tilde{t}_0+\tilde{U}^{(0)}\tilde{L}). \tag{38c, d}$$

The first-order solution for the left-hand side wave (34*a*, *b*) together with (14*a*, *b*) yield the governing equations for the left-hand side motion in the second approximation,

$$\frac{\partial \tilde{u}_l^{(2)}}{\partial \tilde{t}_l}+\frac{\partial \tilde{\rho}_l^{(2)}}{\partial \tilde{x}_l}=-R_0\sin\tilde{x}_l+C_0\sin\tilde{x}_l\cos\tilde{t}_l, \tag{39a}$$

$$\frac{\partial \tilde{\rho}_l^{(2)}}{\partial \tilde{t}_l}+\frac{\partial \tilde{u}_l^{(2)}}{\partial \tilde{x}_l}=B_0\sin\tilde{t}_l\cos\tilde{x}_l, \tag{39b}$$

where

$$\tilde{x}_l=2\alpha\tilde{x},\quad \tilde{t}_l=2\alpha(\tilde{t}-\tilde{t}_0). \tag{39c, d}$$

The constants R_0, C_0, B_0 are

$$R_0=\tfrac{1}{8}(3-\gamma)A^2,\quad C_0=-\tfrac{1}{8}(\gamma-1)A^2,\quad B_0=\tfrac{1}{4}A^2. \tag{40a–c}$$

The boundary conditions (16*a*, *b*) expressed in terms of left-hand side and right-hand side waves are

$$\tilde{u}_{l|_{\tilde{x}=0}}^{(2)}=0,\quad \bar{u}_{r|_{\tilde{x}=\tilde{L}}}^{(2)}=\cos\tilde{t}. \tag{41a, b}$$

Equations (38), (39) together with the boundary conditions (41*a*, *b*), the jump condition (20*b*) and mass normalization condition (21*b*) determine the second approximation. This approximation is discussed in more detail in the following sections.

4.2. *A particular solution*

Using the following simplified notation:

$$\tilde{x}_r\to x,\quad \tilde{t}_r\to t,\quad \tilde{\rho}_r^{(2)}(\tilde{x}_r,\tilde{t}_r)\to\rho_p(x,t),\quad \tilde{u}_r^{(2)}(\tilde{x}_r,\tilde{t}_r)\to u_p(x,t),$$
$$\tilde{x}_l\to x,\quad \tilde{t}_l\to t,\quad \tilde{\rho}_l^{(2)}(\tilde{x}_r,\tilde{t}_r)\to\rho_p(x,t),\quad \tilde{u}_l^{(2)}(\tilde{x}_r,\tilde{t}_r)\to u_p(x,t),$$

(38*a*, *b*) and (39*a*, *b*) may be presented as

$$\frac{\partial u_p(x,t)}{\partial t}+\frac{\partial \rho_p(x,t)}{\partial x}=-R_0\sin x+C_0\sin x\cos t, \tag{42a}$$

$$\frac{\partial \rho_p(x,t)}{\partial t}+\frac{\partial u_p(x,t)}{\partial x}=B_0\sin t\cos x. \tag{42b}$$

A particular solution of the latter system is

$$\rho_p(t,x)=R_0\cos x+R_p(x)\cos t,\quad u_p(t,x)=U_p(x)\sin t, \tag{43a, b}$$

where

$$U_p(x) = \tfrac{1}{4}(C_0 + B_0)\sin x + \tfrac{1}{2}(B_0 - C_0)(x+k)\cos x, \tag{44a}$$

$$R_p(x) = -\tfrac{1}{4}(C_0 + B_0)\cos x - \tfrac{1}{2}(B_0 - C_0)(x+k)\sin x, \tag{44b}$$

with k being a constant to be determined.

Any solution of (38) and (39) may be presented as a sum of a particular solution and a general solution of the homogeneous parts of these equations. The standing-wave-type solution of the homogeneous parts of (38) and (39), which are identical to (23), is

$$\tilde{u}_a = C_a \cos\tilde{t}\sin\tilde{x}, \quad \tilde{\rho}_a = -C_a \sin\tilde{t}\cos\tilde{x}, \tag{45a, b}$$

where C_a is an arbitrary constant. This solution fails to satisfy the condition (41b) at the piston. This condition can only be satisfied by the particular solution (43a, b) and (44a, b), which holds for the right-hand side wave. It can be shown that the particular solution (44) may satisfy the boundary conditions of the problem by a proper choice of the still undetermined constants. Particularly, this solution gives the following expression for the speed of the right-hand side wave:

$$u_r^{(2)}(\tilde{t}_r, \tilde{x}_r) = \sin\tilde{t}_r\,[\tfrac{1}{4}(C_0 + B_0)\sin\tilde{x}_r + \tfrac{1}{2}(B_0 - C_0)(\tilde{x}_r + k_r)\cos\tilde{x}_r],$$

where k_r is an unknown constant. Substitution of this expression together with (39c, d) into (41b) yields

$$\tfrac{1}{2}(B_0 - C_0)k_r \sin 2\alpha(\tilde{t} - \tilde{t}_0 + \pi\tilde{U}^{(0)}) = \cos\tilde{t}. \tag{46}$$

It follows from this equation that

$$\alpha = \tfrac{1}{2}, \quad \tilde{t}_0 = \tfrac{1}{2}\pi, \quad \tfrac{1}{2}(B_0 - C_0)k_r = 1. \tag{47a, c}$$

Note that relations (22) and (47a) provide a proof of assumption (31).

Expressions (36), (37), (22) and (47b) completely determine the speed and the coordinate of the shock front in the zeroth approximation

$$\tilde{U}^{(0)}(\tilde{t}) = \begin{cases} 1 & \text{for} \quad -\tfrac{1}{2}\pi \leqslant \tilde{t} \leqslant \tfrac{1}{2}\pi, \\ -1 & \text{for} \quad \tfrac{1}{2}\pi \leqslant \tilde{t} \leqslant \tfrac{3}{2}\pi \end{cases}, \tag{48a}$$

$$X_u^{(0)}(\tilde{t}) = (\tilde{t} - \tfrac{1}{2}\pi)\,\tilde{U}^{(0)}(\tilde{t}) + \pi. \tag{48b}$$

Now we calculate the first-order terms in expansions (12a, b) and (18b). Bearing in mind relations (22) and (48a, b) we rewrite the solution given by expressions (34a, b) and (35a, b) in the following form:

$$\tilde{u}_l^{(1)} = -\tilde{\rho}_r^{(1)}\tilde{U}^{(0)} = A\sin(\tfrac{1}{2}\tilde{x})\cos(\tfrac{1}{2}\tilde{t} - \tfrac{1}{4}\pi), \tag{49a, b}$$

$$\tilde{u}_r^{(1)} = -\tilde{\rho}_l^{(1)}\tilde{U}^{(0)} = A\tilde{U}^{(0)}\cos(\tfrac{1}{2}\tilde{x})\sin(\tfrac{1}{2}\tilde{t} - \tfrac{1}{4}\pi). \tag{49c, d}$$

Substitution of expressions (48) and (49) into condition (20a) leads to the expression for the shock wave speed:

$$\tilde{U}^{(1)} = \tfrac{1}{4}(3 - \gamma)A\sin\tilde{t}. \tag{50}$$

4.3. *Final results*

The second-order approximation of the left-hand side solution for the velocity and the density is defined by relations (43a, b), (44a, b), (39c, d), (47a, b) and a condition at the plug (41a):

$$\tilde{u}_l^{(2)} = -[\tfrac{1}{4}(C_0 + B_0)\sin\tilde{x} + \tfrac{1}{2}(B_0 - C_0)(\tilde{x}_l + k_l)\cos\tilde{x}]\cos\tilde{t}, \tag{51a}$$

$$\tilde{\rho}_l^{(2)} = R_0\cos\tilde{x} - [\tfrac{1}{4}(C_0 + B_0)\cos\tilde{x} + \tfrac{1}{2}(B_0 - C_0)(\tilde{x} + k_l)\sin\tilde{x}]\sin\tilde{t}, \tag{51b}$$

with

$$k_l = 0. \tag{51c}$$

The second-order approximation of the right-hand side velocity and density solutions is defined by relations (43*a*, *b*), (44*a*, *b*), (38*c*, *d*) and (47*a*, *b*)

$$\tilde{u}_r^{(2)} = -[\tfrac{1}{4}(C_0+B_0)\sin\tilde{x}+\tfrac{1}{2}(B_0-C_0)(x_r-\pi+k_r)\cos\tilde{x}]\cos\tilde{t}, \tag{52a}$$

$$\tilde{\rho}_r^{(2)} = -R_0\cos x-[\tfrac{1}{4}(C_0+B_0)\cos\tilde{x}+\tfrac{1}{2}(B_0-C_0)(\tilde{x}-\pi+k_r)\sin\tilde{x}]\sin\tilde{t}, \tag{52b}$$

with an accuracy to within a constant k_r.

The unknown constant k_r may be calculated from the condition on the shock front (20*b*). For this purpose we substitute expressions (48)–(52) into condition (20*b*) leading to the following equation:

$$\tfrac{1}{2}(B_0-C_0)(k_r-\pi)\,\tilde{U}^{(0)}\sin(2\tilde{t}) = 0. \tag{53}$$

Combining this with (47*c*) one can calculate the constant k_r

$$k_r = \pi. \tag{54}$$

Simple calculations using expressions (40*b*, *c*), (47*c*) and (54) also yield the parameter A.

$$A = \frac{4}{((\gamma+1)\pi)^{1/2}}. \tag{55}$$

This parameter completely determines the first-order solution (49) and (50).

The second-order solution which is given by relations (51*a*, *c*), (52*a*, *b*), (54), (40*a*–*c*) and (55) may finally be written as:

$$\tilde{u}_l^{(2)} = \tilde{u}_r^{(2)} = -\left[\frac{\tilde{x}}{\pi}\cos\tilde{x}+B\sin\tilde{x}\right]\cos\tilde{t} = \tilde{u}^{(2)} \quad \text{(say)}, \tag{56a, b}$$

$$\tilde{\rho}_r^{(2)}+4B\cos\tilde{x} = \tilde{\rho}_l^{(2)}-4B\cos\tilde{x} = -\left[\frac{\tilde{x}}{\pi}\sin\tilde{x}+B\cos\tilde{x}\right]\sin\tilde{t} = \tilde{\rho}^{(2)} \quad \text{(say)}, \tag{57a, b}$$

where

$$B = \frac{3-\gamma}{2\pi(\gamma+1)}. \tag{58}$$

It is seen from expressions (56) and (57), that in the second approximation the gas speed is a continuous function, while the expression for its density includes continuous and discontinuous parts. Let us clarify the physical sense of these parts. Using the second-order solution given by expressions (57*a*, *b*) together with the shock wave coordinate defined by relation (48*b*) one can calculate:

$$\sin\tilde{t}+\int_0^{\pi}\tilde{\rho}^{(2)}(\tilde{t},\tilde{x})\,\mathrm{d}\tilde{x} = 0, \tag{59a}$$

$$\int_0^{\tilde{X}_u^{(0)}(\tilde{t})} 4B\cos\tilde{x}\,\mathrm{d}\tilde{x}-\int_{\tilde{X}_u^{(0)}(\tilde{t})}^{\pi} 4B\cos\tilde{x}\,\mathrm{d}\tilde{x} = 8B\tilde{U}^{(0)}\cos\tilde{t}. \tag{59b}$$

The sum of the left-hand sides of expressions (59*a*) and (59*b*) represents the left-hand side of (21*b*). Expression (59*a*) merely states that the continuous part of the solution describes a density oscillation caused by the piston. The discontinuous part of the

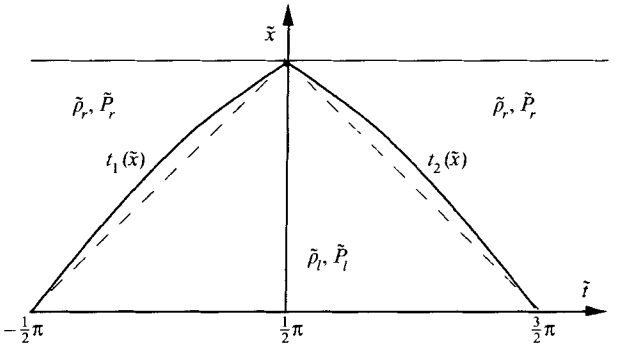

FIGURE 3. The time averaging procedure.

second-order solution is presented by expression (59*b*). It is due to the nonlinear terms appearing in the right-hand side of (21*b*).

The right-hand side of (21*b*) is a product of the density jump at the shock front in the zeroth approximation, $X_u^{(0)}(\tilde{t})$, and the first approximation of the shock front coordinate $X_u^{(1)}(\tilde{t})$. Using expressions (48*b*) and (49) we obtain an expression for the density jump:

$$\tilde{\rho}_l^{(1)}(\tilde{t}, \tilde{X}_u^{(0)}(\tilde{t})) - \tilde{\rho}_r^{(1)}(\tilde{t}, \tilde{X}_u^{(0)}(\tilde{t})) = -A\tilde{U}^{(0)}. \tag{60}$$

This expression merely states that the density jump is equal to $-A$ on the shock wave propagating from the left to the right and A on the shock wave propagating from the right to the left.

Substitution of expressions (59*a*, *b*) into the mass normalization condition (21*b*) yields the first approximation of the shock front coordinate as:

$$X_u^{(1)}(\tilde{t}) = -8\left(\frac{B}{A}\right)\cos\tilde{t}. \tag{61}$$

This expression together with (37) determine the shock-front coordinate (18*b*) up to the terms of second order with respect to the small parameter ϵ. Figure 3 shows by bold curves the first-order approximation of the shock-front trajectory while the zeroth approximation is shown by dashed lines. One can see that the contribution of the first-order approximation (61) distorts the shock-wave trajectory but does not change the time of the reflection of the shock front which is determined by the zeroth-order solution.

5. Discussion

The form of the present solution for the speed and density of the gas (34) and for the shock speed (36), (50) was first proposed by Betchov (1958). However, his study did not consider the reflection of the shock wave from the piston or the plug. Betchov considered the continuous parts of the solution for the left-hand side and right-hand side waves and did not calculate the magnitude of the jump as given by the parameter A. The complete form of the first-order solution (49) and (55) was obtained by Chester (1964). In the present study we have augmented the solution by the second-order terms (56*a*, *b*) and (57*a*, *b*). Below, we discuss the effects of these new additional terms.

Some idea of the influence of the nonlinear terms can be obtained from the data given by Saenger & Hudson (1960) for a tube of length $L = 67$ in., a piston amplitude $l = 0.125$ in., and the resultant first resonance frequency $f_r = 100.6$ Hz. From these data

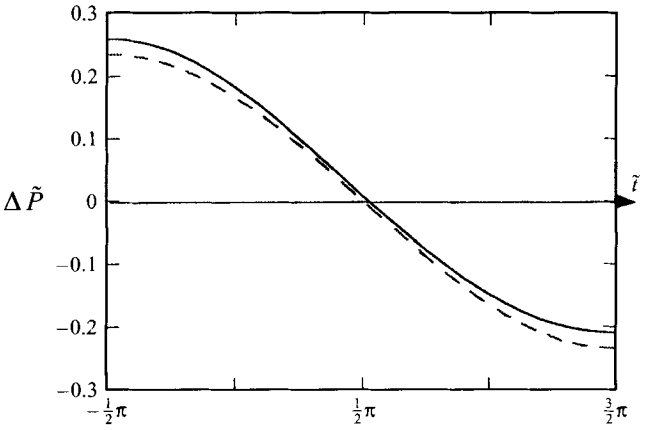

FIGURE 4. Pressure oscillations at the closed end of the tube. Dashed line corresponds to the theory of Chester, continuous line corresponds to the present theory.

one finds $\epsilon = 0.077$. Setting $\gamma = 1.4$ and using (55) and (57) one obtains for air the following values of the parameters: $A = 1.46$, $B = 0.106$. Chester's solution for these conditions, as given by expressions (49*b*, *d*) and the present nonlinear solution given by expressions (57*a*, *b*) and (58) may be substituted into equation (12*c*) to obtain the pressure oscillations during the experiment. Comparison of the results of these two solutions enables us to assess the effect of the additional terms on the pressure, as shown in figure 4. One can see that for these experimental conditions the deviation of Chester's theory from ours does not exceed 5%. Moreover, both these theories give the same pressure change at the closed end of the resonance tube, namely about of 23.5 cm Hg. This value differs from the experimental data of Saenger & Hudson (1960) by about 8%.

However, there are two important differences between Chester's theory and ours. First, Chester's theory predicts the average gas pressure to be equal to the initial pressure, while the present theory predicts an increase in the time averaged pressure at the plug owing to the oscillations of the piston. This result agrees qualitatively with the experimental data of Saenger & Hudson (1960), as shown in their figure 1(*d*), Zaripov & Ilhamov (1976) as shown in their figure 7 and Merkli & Thomann (1975), as shown in their figure 6(*b*). Secondly, the present theory predicts that there exists an average pressure gradient along the tube. This is confirmed by the data presented in figure 6(*b*) of Merkli & Thomann (1975).

In order to verify these two effects we average the solution obtained. Using expressions (12*a*, *c*) the time averaged pressure and density disturbances of the quiescent gas are obtained

$$\Delta\tilde{\rho}_{av} = \epsilon\tilde{\rho}^{(1)}_{av} + \epsilon^2\tilde{\rho}^{(2)}_{av}, \tag{62a}$$

$$\Delta\tilde{P}_{av} = \epsilon\tilde{\rho}^{(1)}_{av} + \epsilon^2\tilde{\rho}^{(2)}_{av} + \tfrac{1}{2}(\gamma-1)\,\epsilon^2[(\tilde{\rho}^{(1)})^2]_{av}, \tag{62b}$$

where the time averaging scheme may be expressed via the left-hand side and right-hand side solutions as follows:

$$\xi_{av} \equiv \int_{-\pi/2}^{3\pi/2} \xi(\tilde{x},\tilde{t})\,\mathrm{d}\tilde{t} = \int_{-\pi/2}^{t_1(\tilde{x})} \xi_l(\tilde{x},\tilde{t})\,\mathrm{d}\tilde{t} + \int_{t_1(\tilde{x})}^{t_2(\tilde{x})} \xi_r(\tilde{x},\tilde{t})\,\mathrm{d}\tilde{t} + \int_{t_2(\tilde{x})}^{3\pi/2} \xi_l(\tilde{x},\tilde{t})\,\mathrm{d}\tilde{t}, \tag{63}$$

where $\xi(\tilde{x},\tilde{t})$ is an arbitrary function of $\tilde{x}$, $\tilde{t}$; and $t_1(\tilde{x})$, $t_2(\tilde{x})$ are successive times of shock

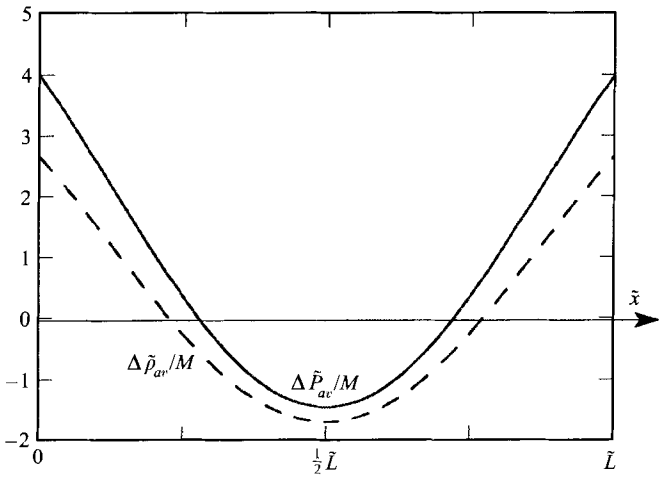

FIGURE 5. The time averaged pressure and density distributions.

wave passage through the section with the coordinate $\tilde{x}$ (see figure 3). During one oscillation period the shock wave passes twice through any section of the tube. The times $t_1(\tilde{x})$, $t_2(\tilde{x})$ of the shock wave passage are the solutions of the equation

$$\tilde{X}_u(\tilde{t}(\tilde{x})) = \tilde{x}. \tag{64}$$

The left-hand side of the latter equation is determined by expressions (18*b*), (48*b*) and (61) with an accuracy up to the first order with respect to the small parameter ϵ. With the same accuracy asymptotic solutions of (64) are given by

$$t_1(\tilde{x}) = \tilde{x} - \tfrac{1}{2}\pi + 8\left(\frac{B}{A}\right)\epsilon\sin\tilde{x}, \quad t_2(\tilde{x}) = \tfrac{3}{2}\pi - \tilde{x} + 8\left(\frac{B}{A}\right)\epsilon\sin\tilde{x}, \tag{65a, b}$$

where the first two terms on the left-hand side correspond to the zeroth approximation and the last term to the first approximation. Taking these expressions together with the first- and second-order solutions for density, given by expressions (49*b*, *d*), and (57*a*, *b*), respectively, and using the definition (63) one can calculate:

$$\tilde{\rho}_{av}^{(1)} = -16B\epsilon\sin\tilde{x}, \quad \tilde{\rho}_{av}^{(2)} = 8B(\pi - 2\tilde{x})\cos\tilde{x}, \tag{66a, b}$$

$$[(\tilde{\rho}^{(1)})^2]_{av} = A^2[(\pi - \tilde{x})\cos\tilde{x} + \pi\sin^2(\tfrac{1}{2}\tilde{x}) - \sin\tilde{x}], \tag{66c}$$

where A and B are given by (55) and (58), respectively. Substitution of (66*a*, *b*) into (62*a*, *b*) yields the average density distribution, while a proper combination of expressions (66*a*–*c*) yields the average pressure distribution. For the special case of the tube used by Merkli & Thomann (1975) these two distributions are presented in figure 5. As can be seen, the present theory predicts a minimum average density as well as a minimum average pressure around the middle section of the tube. The latter prediction agrees with the experimental data of Merkli & Thomann (1975), as seen in their figure 6(*b*).

We now compare the analytical result for the averaged pressure, given by (62*b*) and (66*a*–*c*), with the measurements of Saenger & Hudson (1960). They obtained at the closed end of the tube an average pressure of 18.5 cm H_2O. For the same conditions, the present theory yields $\Delta P_{av} = 4\gamma\epsilon^2 P_0 = 32.8$ cm H_2O with P_0 being the atmospheric pressure. The difference between theoretical and experimental results of the averaged pressure may be explained by: (i) rather low accuracy of the data of Saenger &

Hudson; (ii) the fact that the theory neglects gas viscosity, which reduces the shock waves strength and, hence, all effects connected with the waves; (iii) small changes of the resonant frequency caused by entropy variations during the experiment.

Indeed, for the experimental conditions of Saenger & Hudson (1960) given in their paper, $f_r \sim 0.01\ s^{-1}$, $\epsilon \sim 0.077$, the characteristic timescale for $O(\epsilon)$-entropy changes is just about $\epsilon^{-2}/f_r \approx 0.6$ s. It is possible that the experiment has been run at least as long as this. On the other hand, the inviscid solution predicts pressure changes at the closed end of the tube of about 23.5 cm Hg while Saenger & Hudson (1960) measured 21.6 cm Hg. The error of the inviscid solution (1.9 cm Hg which is about 25 cm H_2O) was attributed by Chester (1964) to the shear viscosity. This error is of the same order as the difference in the average pressure between present theory and the experimental data.

The above analysis shows that nonlinear terms lead to pressure gradients in resonant tubes, although viscosity and entropy effects may modify the magnitude of this phenomenon.

6. Conclusions

The existence of a pressure minimum within the tube was experimentally confirmed by Merkli & Thomann (1975) for the case of a shockless piston oscillation. When the frequency of the piston oscillation, f, is far from the resonance frequency, f_r the spatial inhomogeneous terms are of order M^2 and much smaller than the amplitude of the pressure oscillation, which is of order M. In the case of resonance oscillations, considered in the present study, the amplitude of the pressure oscillation is of order $M^{1/2}$, while the spatial inhomogeneous terms are of order M (see expressions (62) and (66)). Hence, in the resonance case the pressure gradient is significantly larger than in the case of regular acoustic oscillations. This effect is of considerable scientific and engineering interest, since it should intensify all transport processes inside the oscillating tube. For example, we expect that this effect can be used to enhance small particle drift under the influence of acoustic waves.

This research was supported by the Fund for the Promotion of Research at the Technion and by the Israel Science Foundation Grant 529-93-1.

REFERENCES

BETCHOV, B. 1958 Non-linear oscillations of the column of a gas. *Phys. Fluids* **1**, 205–212.

CHESTER, W. 1964 Resonant oscillations in closed tubes. *J. Fluid Mech.* **18**, 44–64.

CRUIKSHANK, D. B. 1972 Experimental investigation of finite-amplitude acoustic oscillations in a closed tube. *J. Acoust. Soc. Am.* **52**, 1024–1036.

GALIEV, SH. U., ILHAMOV, M. A. & SADYKOV, A. V. 1970 Gas periodic shock waves. *Izv. Akad. Nauk. SSR Mech. Jidcosty i Gasa* **2**, 57–66.

KELLER, J. 1976 Resonant oscillations in closed tubes: The solution of Chester's equation *J. Fluid Mech.* **77**, 279–304.

KLEIN, R. & PETERS, N. 1988 Cumulative effects of weak pressure waves during the induction period of a thermal explosion in a closed cylinder. *J. Fluid Mech.* **187**, 197–230.

MAJDA, A. & ROSALES, R. 1984 Resonantly interacting, weakly nonlinear, hyperbolic waves. I. A single space variable. *Stud. Appl. Maths* **71**, 149–179.

MAJDA, A., ROSALES, R. & SCHONBEK, M. 1988 A canonical system of integrodifferential equations arising in resonant nonlinear acoustics. *Stud. Appl. Maths* **79**, 205–262.

MERKLI, P. & THOMANN, H. 1975 Thermoacoustic effects in a resonance tube. *J. Fluid Mech.* **70**, 161–177.

OCKENDON, H., OCKENDON, J. R., PEAKE, M. R. & CHESTER, W. 1993 Geometrical effects in resonant gas oscillations. *J. Fluid Mech.* **77**, 61–66.

OCHMANN, M. 1985 Nonlinear resonant oscillations in closed tubes – An application of the averaging method. *J. Acoust. Soc. Am.* **32**, 961–971.

SAENGER, R. A. & HUDSON, G. E. 1960 Periodic shock waves in resonating gas columns. *J. Acoust. Soc. Am.* **32**, 961–971.

WANG, M. & KASSOY, D. R. 1990 Evolution of weakly nonlinear waves in a cylinder with a movable piston. *J. Fluid Mech.* **221**, 23–52.

WANG, M. & KASSOY, D. R. 1995 Nonlinear oscillations in a resonant gas column: an initial-boundary-value study. *SIAM J. Appl. Maths* **55**, 923–951.

ZARIPOV, R. G. & ILHAMOV, M. A. 1976 Non-linear gas oscillations in a pipe. *J. Sound Vib.* **46**, 245–257.